Progress In Electromagnetics Research, Vol. 134, 437–454, 2013

HIGH PERFORMANCE MULTI-SECTION CORRUGATED SLOT-COUPLED DIRECTIONAL COUPLERS

Alvaro Moscoso-Martir*, **Inigo Molina-Fernandez**, and **Alejandro Ortega-Monux**

Departamento de Ingenieria de Comunicaciones, ETSI Telecomunicacion, Malaga University, Campus Universitario de Teatinos s/n, Malaga 29011, Spain

Abstract—In this paper a robust technique for the design of high performance directional couplers is proposed. It combines the advantages of wiggly coupled lines and slot-coupled lines but overcomes their main limitations. The key to this novel technique is a new corrugated slot that allows perfect compensation of the even and odd mode phase velocities and can be easily designed using Bloch-Floquet theory, yielding outstanding performance. To demonstrate the validity of the proposed technique, the design of two different wideband directional couplers is presented. The first design consists of a 10 dB asymmetric directional coupler with a one decade bandwidth (1.2–12 GHz) that exhibits a coupling accuracy of 10 ± 0.6 dB, a return loss better than 23 dB and an isolation better than 28 dB across the complete frequency band. The second design consists of a symmetric quadrature hybrid that operates over the complete UWB band (3.1 to 10.6 GHz) showing an amplitude and phase imbalance between the output ports lower than ± 0.5 dB and $\pm 0.7^\circ$, respectively.

1. INTRODUCTION

Directional couplers are essential passive components of many microwave systems. They are used either in a symmetrical or asymmetrical configuration depending on the specific application. The symmetrical configuration is useful in systems where a specific phase performance is required (such as modulators, balanced amplifiers and mixers, network analyzers, etc.), and the asymmetrical configuration is used in systems where the phase performance is irrelevant (such us power meters, source leveling and test systems).

Received 15 November 2012, Accepted 1 December 2012, Scheduled 6 December 2012

* Corresponding author: Alvaro Moscoso-Martir (amm@ic.uma.es).

Buried homogeneous structures are particularly well suited to directional coupler design, as they support TEM modes with the same phase velocity [1]. However, they are not well suited to hybrid integration of components, as the transitions required for accessing to the external metal layers usually degrade their potential performance. Hence, the design of these couplers in microstrip compatible technologies is of great interest. The main difficulties in realizing high performance and wideband directional couplers in microstrip technology are: i) obtaining tight coupling, ii) compensating for the parasitics of the discontinuities between coupled sections, and iii) equalizing phase velocities of even and odd modes in the complete operation bandwidth.

In coupled microstrip lines, several techniques have been proposed to overcome these difficulties: reentrant mode directional couplers [2], patterned ground plane directional couplers [3], inductively compensated couplers [4], directional couplers with grooved substrates [5], directional couplers with dielectric overlay [6], modified vertically installed planar couplers [7], rat-race couplers [8], non-uniform couplers [9, 10], etc.. However, these techniques cannot completely compensate even and odd mode phase velocities as they partially affect both modes field patterns or require complete redesign of circuits. Furthermore, wiggly coupled lines has been also proposed in non-uniform [11] and multi-section directional couplers [12–14] for phase velocity equalization. Wiggling the adjacent edges of the microstrip lines slows down the odd mode phase velocity without greatly affecting the even mode, equalizing their phase velocities. However, this technique suffers from two main limitations: i) phase equalization is limited as the even mode is also affected by the wiggled edges [11, 12], and ii) edge-coupled microstrip lines cannot achieve the tight coupling required for wideband directional couplers. This lack of coupling has been partially resolved using tandem structures with interdigital couplers in their central section [11, 13]. However, even in these cases, the proposed structures require substrates of high dielectric constant (such as Alumina) to achieve tight coupling with strip and gap widths which can actually be manufactured.

A useful structure for solving some of the aforementioned problems is the slot-coupled directional coupler [15], which can easily achieve tight coupling. However, the parasitic effects of the discontinuities and the difference between the even and odd mode phase velocities limit its operational bandwidth. To solve these limitations, a slot-coupled multi-section quadrature hybrid was presented in [16], in which the lengths of the different sections were modified to adjust coupler performance. Also, elliptically shaped slot-coupled quadrature couplers [17] and coplanar waveguide slot-coupled directional couplers [18] have been proposed. Even though all these solutions are valid for frequency bands up to two octaves, their performance is clearly degraded in larger slot-coupled multi-section structures that cover wider frequency bands.

In this paper a new technique combining the main advantages of the wiggly coupled lines with the advantages of the slot-coupled directional coupler is proposed. This makes use of a novel corrugated slot in the ground plane that completely equalizes both mode phase velocities even in tightly coupled sections where their differences are considerable. Besides, as it will be shown in Section 3, the introduction of corrugations in the slot does not significantly affect the modal impedances. Therefore, this technique makes it possible to develop a more robust design strategy than previously reported methods [2, 3, 5, 6, 11], since it allows the phase velocity equalization problem to be decoupled from the classical TEM coupler design based on the selection of adequate impedance values for the sections.

To assess the validity of the proposed technique, the design of two high performance directional couplers in Rogers 4350B substrate (610 μm thickness, $\epsilon_r = 3.66$) is presented. The first one is a 10 dB asymmetric five-section slot-coupled directional coupler, that operates from 1.2 to 12 GHz. It offers a high coupling accuracy of 10 ± 0.6 dB and return loss and isolation better than 23 dB and 28 dB respectively, improving previously reported results in terms of fractional bandwidth and performance [2, 4–6]. The second one is a three-section symmetric quadrature hybrid similar to the coupler recently used to realize a high performance six-port IQ demodulator with full UWB coverage [19]. This circuit presents a return loss better than 22 dB, an isolation better than 26 dB, a coupling level of -3 ± 0.5 dB and a phase response of $90 \pm 0.7^\circ$ from 3.1 to 10.6 dB, cleary outperforming previously reported results [3, 7, 16–18].

The scope of the paper is as follows. In Section 2, the slot-coupled directional coupler design procedure will be reviewed. This procedure will be used in subsequent sections to obtain an initial guess for the proposed technique for high performance corrugated couplers design. In Section 3, the corrugated slot technique (based on Bloch-Floquet mode analysis) is presented and applied to design the 10 dB coupler. In Section 4, this technique will be applied to design the high performance wideband 3 dB hybrid. Finally, the conclusions will be presented in Section 5.

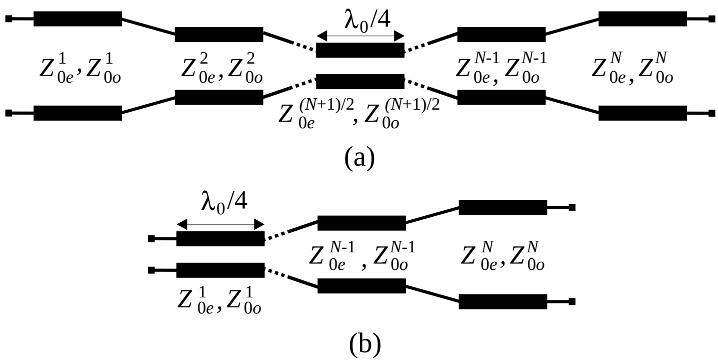

Figure 1. Multisection directional coupler circuital diagram. (a) Symmetric configuration. (b) Asymmetric configuration.

2. DIRECTIONAL COUPLER DESIGN BASED ON MODAL ANALYSIS (2D)

In this section we explain the design procedure used to calculate the initial dimensions of a slot-coupled directional coupler and assess the difference between the even and odd mode phase velocities.

A multisection equal-ripple directional coupler is a circuit with an arbitrary number of sections in which each section is designed to be a quarter wavelength at the central frequency (see Figure 1), with a pair of even-odd mode impedances that can be found in tables in [20, 21]. If the coupling structure can support two pure TEM modes (even and odd modes), this procedure allows an straightforward design of multisection TEM directional couplers for an ideal situation. However, in practice second order effects (such as discontinuity parasitics, quasi-TEM mode character, or dispersion) can make the design flow somewhat more complicated, making it a challenge to obtain wideband operation with reasonable isolation values.

A slot-coupled directional coupler consists of two microstrip lines coupled through a rectangular slot in their common ground plane as shown in Figure 2(a). This structure does not support true TEM modes, so in its design is crucial to consider not only the effects of the discontinuities, but also the difference between phase velocities of even and odd modes.

In the slot coupler, the even and odd modes are intrinsically orthogonal. Hence, it is possible to model and simulate the propagation of both modes separately, using the equivalent circuits shown in Figure 2(b). Then, the final coupler behavior can then be recovered

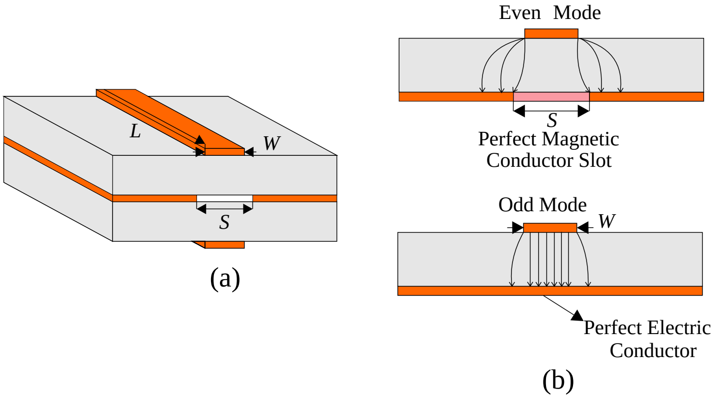

Figure 2. (a) 3D microstrip slot coupling structure. (b) Even-mode and odd-mode equivalent circuits.

combining their even ($[S]_e$) and odd ($[S]_o$) scattering parameters matrices [22–24]:

$$[M] = \frac{1}{\sqrt{2}} \begin{bmatrix} I & I \\ -I & I \end{bmatrix} \tag{1}$$

$$[S]_c = \begin{bmatrix} [S]_{dd} & [S]_{dc} \\ [S]_{cd} & [S]_{cc} \end{bmatrix} = \begin{bmatrix} [S]_e & 0 \\ 0 & [S]_o \end{bmatrix} \tag{2}$$

$$[S]_{coupler} = [M]^{-1} [S]_c [M] \tag{3}$$

In the proposed modal analysis (2D) design flow (shown in Figure 3) the initial values for the even and odd mode characteristic impedances (Z^i_{0e}, Z^i_{0o}) of each section are obtained from tables included in [20, 21]. With these characteristic impedances, initial values for the width of the tracks (W_i) and slots (S_i) in each section are calculated using the approximate analytical closed-form expressions obtained using conformal mapping techniques in [25]. However, it has been noticed by numerical 2D modal analysis for the different sections that the even and odd mode characteristic impedances of the structure for these initial dimensions usually differ from the desired impedance values. Hence, a 2-D modal optimization of both modes for each section must be performed to adjust (W_i, S_i) and get the expected characteristic impedances. In doing so, the values of the effective permittivities ($\varepsilon^i_{eff_e}$, $\varepsilon^i_{eff_o}$) are also obtained.

Once the initial values of the structure (W_i, S_i, $\varepsilon^i_{eff_e}$, $\varepsilon^i_{eff_o}$) have been calculated, the directional coupler response can be simulated to determine the effect of the difference between the even and odd mode phase velocities.

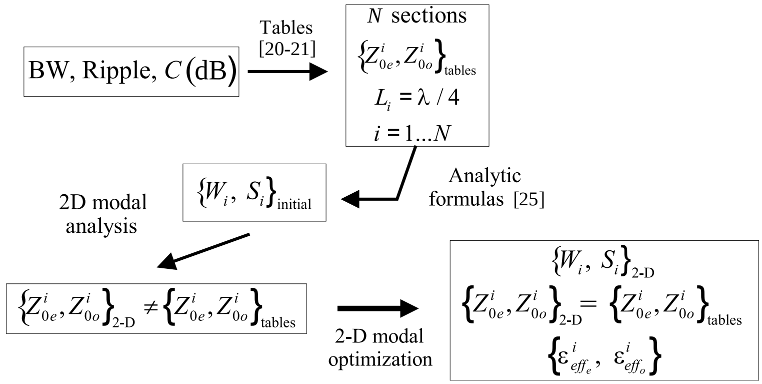

Figure 3. Diagram of the initial modal analysis (2D) design flow.

3. DESIGN AND EVALUATION OF A FIVE-SECTION 10 dB ASYMMETRIC SLOT-COUPLED DIRECTIONAL COUPLER

In this section, we present the realization of a one decade bandwidth 10 dB asymmetric slot-coupled five-section directional coupler, which makes use of the new corrugated slot to improve its performance. To make clear the advantages of this proposal, we will first carry out a classical non-corrugated design, and then we will present the proposed technique and assess its performance.

3.1. Classical-slot Coupler Design

In this type of wideband weakly coupled structures, the difference between the even and odd mode phase velocities completely degrades the directional coupler performance. However, the small coupling required makes the parasitic effects of discontinuities between the sections almost negligible and easy to compensate slightly adjusting the length of the sections.

According to the 2-D modal analysis of Figure 3, the specific impedances for this design and the coupling level of each section (included in [21]) are obtained (see Table 1). Then, the track and slot widths of each section (W_i, S_i) are optimized to get these target impedance values.

The results of the cross-sectional dimensions and the effective permittivities for the proposed directional coupler are given in Table 2. Analyzing these results, it is clear that there is a significant difference between the effective permittivities of both modes with a relative error

Table 1. Even-odd mode characteristic impedances (Z_{0e}^i, Z_{0o}^i) and coupling level of each section for the five-section asymmetric 10 dB directional coupler obtained from [20].

Section	1	2	3	4	5
Z_{0e} (Ω)	88.06	74.56	65.21	58.79	54.51
Z_{0o} (Ω)	28.39	33.53	38.34	42.52	45.86
C (dB)	-5.8	-8.4	-11.7	-15.9	-21.3

Table 2. Cross-sectional dimensions (W_i, S_i) and even-odd mode effective permittivities ($\varepsilon^i_{eff_e}$, $\varepsilon^i_{eff_o}$) for each section at 6.6 GHz (central frequency band) obtained by modal optimization based on 2-D analysis.

Section	1	2	3	4	5
W(mm)	1.51	1.2	0.97	0.83	0.74
S(mm)	2	1.38	0.95	0.65	0.43
ε_{eff_o}	2.97	2.91	2.86	2.82	2.79
ε_{eff_e}	2.10	2.29	2.48	2.61	2.69

of a 30% in the first section (the worst case); this means a relative error higher than 19.5% between the physical length required for the even and odd modes (L_e^1, L_o^1) to be a quarter wavelength. With these initial values, the simulation of the structure shows an extremely poor isolation and return loss as is depicted in Figure 4, which cannot be compensated without modal phase velocity equalization.

3.2. Corrugated-slot Coupler Design

In this work we propose the introduction of a corrugated slot to equalize the even and odd mode phase velocities. In this technique, inspired by the wiggly coupled lines [12, 14], rectangular shaped teeth (of width T_i and depth D_i), smaller than the wavelength at the central frequency (i.e., smaller than 100–300 µm in our case), are added to the edge of the slots in the different sections, as shown in Figure 5. These corrugations have a period Λ_i and a duty cycle $\eta_i = T_i/\Lambda_i$. The introduction of these corrugations increases the electrical length of the even mode, but it does not affect the odd mode (i.e., Z_{0o}^i, $\varepsilon^i_{eff_o}$, W_i and L_o^i remain unchanged). Therefore, if the geometry of the teeth is properly designed, it is possible to achieve a nearly perfect

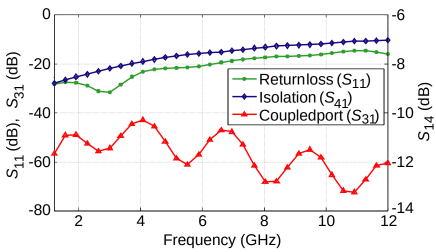

Figure 4. Electromagnetically adjusted performance of the 10 dB directional coupler.

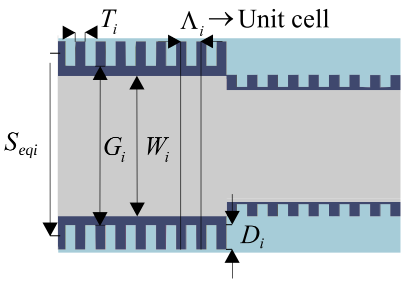

Figure 5. Detailed plot of a piece of the coupler between two sections showing the upper and lower tracks (grey) coupled through the corrugated slot (blue).

phase velocity equalization (i.e., $\varepsilon^i_{\mathit{eff}_o} = \varepsilon^i_{\mathit{eff}_e}$) without greatly affecting the characteristic impedances of the previously designed directional coupler sections. Since the proposed structure used for the even mode consists of a periodic repetition of rectangular shaped teeth, as depicted in Figure 5, we will use the Bloch-Floquet analysis [26, 27] to perform a rigorous calculation of characteristic impedances and propagation constants for the even mode.

Using the HFSS eigenmode solver with master/slave boundary conditions, it is possible to simulate only a unit cell of the periodic structure (for each section) for different periods Λ_i and depths D_i of the rectangular teeth. These simulations enable calculation of the periodic structure resonant frequency (f^i_r) as a function of the phase delay (ϕ_i) introduced by the unit cell. With f^i_r, the new and compensated even mode effective permittivity for each section ($\varepsilon^i_{\mathit{eff}_e}$) can be easily calculated as:

$$\varepsilon^i_{\mathit{eff}_e} = \left(\frac{\phi_i\, c}{2\pi f^i_r \Lambda_i}\right)^2 \tag{4}$$

where c is the speed of light in vacuum.

A major problem is the calculation of the characteristic impedance of the periodic structure. The characteristic impedance of an infinite periodic structure is assumed to be the Bloch impedance (Z_B) at the unit cell terminals [26, 27]. However, as the Bloch mode field pattern is not constant along the period, the Bloch impedance can change depending on the position where the unit cell terminals are fixed. If this occurs, a unique Bloch impedance cannot be defined for each section.

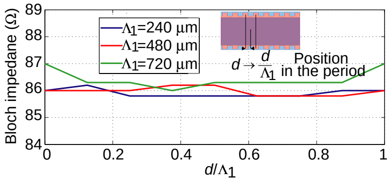

Figure 6. Calculated even mode Bloch impedance of the first section fixing the beginning of the unit cell in several positions of the period (d/Λ_1). ($D_1 = 280\,\mu\text{m}$, $G_1 = 1.72\,\text{mm}$ and $\eta = 0.5$).

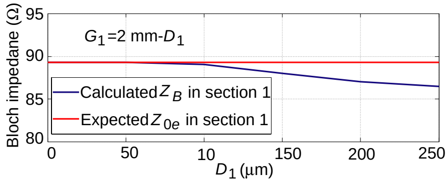

Figure 7. Calculated even mode Bloch impedance for the first section of the directional coupler as a function of D_1 with $\eta = 0.5$, $\Lambda_1 = 240\,\mu\text{m}$ and keeping the equivalent slot width (S_{eq1}) constant to $2\,\text{mm}$ (i.e., setting $G_1 = 2\,\text{mm} - D_1$).

Fortunately, this is not the case, as it has been shown that the Bloch impedance Z_B barely changes when it is calculated in different cross-sectional cuts along the unit cell. This is illustrated in Figure 6 where the Bloch impedance of the first corrugated section of the coupler ($D_1 = 280\,\mu\text{m}$, $G_1 = 1.72\,\text{mm}$ and $\eta = 0.5$) is calculated fixing the beginning of the unit cell in several positions d/Λ_1 of the period. Results are plotted for three different periods. It can be seen that impedance of the Bloch mode is almost independent of the position where it is calculated. On the other hand, Figure 6 also shows that the Bloch impedance does not change significantly with the period.

It has been observed that for $\eta = 0.5$ and for a broad range of corrugation depths (D_i), the even mode Bloch impedance of the corrugated structure is always close to the even mode impedance of a z-invariant coupled slot section of equivalent width S_{eqi} such that

$$S_{eqi} = G_i + D_i = S_i \tag{5}$$

This is shown in Figure 7 where the even mode Bloch impedance of the first section is calculated for different corrugation depths (D_1) while keeping S_{eq1} fixed to the value of Table 2 ($S_{eq1} = 2\,\text{mm}$), ensuring a value close to $Z_{oe1} = 88.06\,\Omega$ of Table 1. It is observed that while satisfying (5), the Bloch impedance value is only slightly modified when the teeth depth is increased ($86\,\Omega$ in the worst case). Hence, fixing (5) as a design criterion, the teeth depth and period can be used to equalize the phase velocities of the modes without greatly affecting the impedance of the section. It allows the phase velocity equalization problem to be decoupled from the impedance design problem, thus making the design strategy robust.

Effectively, as W_i and S_{eqi} are known from the 2-D modal analysis performed in Section 2, the only unknown dimensions to be obtained

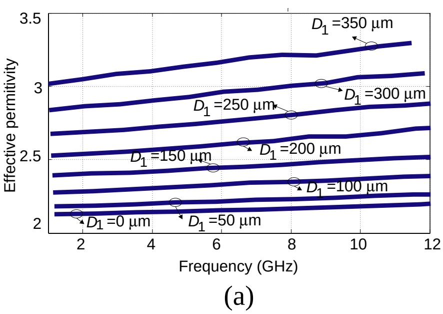

Figure 8. Even mode effective permittivities of the first section ($\varepsilon^1_{eff_e}$) for different teeth depths (D_1) assuming $\eta = 0.5$ and $G_1 = 2\,\text{mm} - D_1$ (5). (a) $\Lambda_1 = 240\,\mu\text{m}$. (b) $\Lambda_1 = 480\,\mu\text{m}$.

by simulation are the depths (D_i) and periods (Λ_i) of the rectangular teeth in each section. Hence, performing fast simulations of only one unit cell as a function of D_i for two or three periods (Λ_i), the values for equalizing both mode phase velocities (i.e., $\varepsilon^i_{eff_o} = \varepsilon^i_{eff_e}$) are easily obtained.

In Figure 8 the specific results obtained for the first section (the worst case) are shown. Analysing Figure 8(a), with $\Lambda_1 = 240\,\mu\text{m}$ a teeth's depths of $300\,\mu\text{m}$ is sufficient to attain the required value of $\varepsilon^1_{eff_e} = 2.97$ (see Table 2) and thus to compensate both modes at 6.6 GHz. However if $\Lambda_1 = 480\,\mu\text{m}$, a higher teeth's depths of $350\,\mu\text{m}$ is required to achieve the same effective permittivity, as shown in Figure 8(b). Carrying out these type of simulations in all the sections of the directional coupler, the required D_i and Λ_i in all the corrugated sections can be directly obtained in a computationally efficient manner.

Once every dimension of the directional coupler has been calculated, only minor corrections of the geometrical parameters (lower than 5%) are required to account for second order effects as the finite thickness of the conductors. This is done by means of 3D electromagnetic simulation.

The previous design procedure has been applied to the 10 dB directional coupler. The periods (Λ_i) of all the sections were set to $240\,\mu\text{m}$, except for Section 4 ($\Lambda_4 = 580\,\mu\text{m}$). In the case of Section 4, the simulations showed that it required a very small phase velocity correction. Therefore, Λ_4 was increased to make the rectangular teeth's depths fabricable (the minimum fabricable track/gap size is $100\,\mu\text{m}$ for our technology). The remaining final dimensions of the directional coupler are shown in Table 3.

To verify the directional coupler's performance within operation

Table 3. Physical dimensions of the 10 dB five section directional coupler.

Sections	1	2	3	4	5
W (mm)	1.57	1.25	1.02	0.86	0.76
L (mm)	6.43	6.53	6.62	6.64	6.68
S (mm)	2.07	1.45	1.01	0.69	0.47
D (µm)	280	140	100	100	100
Λ (µm)	240	240	240	580	240

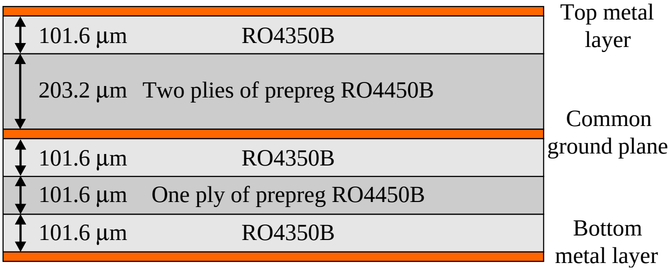

Figure 9. Symmetrical multilayer stack made with RO4350B substrate.

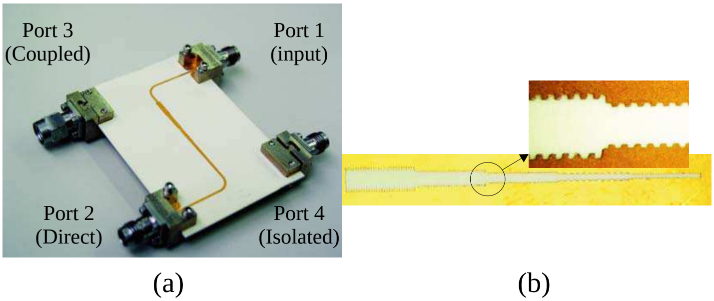

Figure 10. (a) Photograph of the 10 dB five-section directional coupler. (b) Photograph of the inner corrugated slot plane.

bandwidth (1.2–12 GHz), a prototype has been manufactured using the symmetrical multilayer stack shown in Figure 9. A photograph of the fabricated directional coupler and its novel corrugated slot is shown in Figure 10. The directional coupler has been measured with a two-port VNA using 2.4 mm Southwest connectors and a TRL calibration technique. The unused ports of the coupler were loaded with coaxial matched terminations.

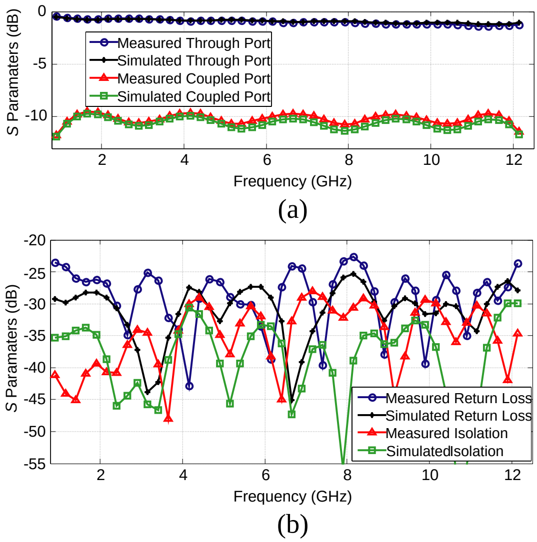

Figure 11. Measured and simulated performance of the fabricated five-section directional coupler. (a) Through and coupled ports. (b) Return loss and isolation.

Figure 11 shows the electromagnetically simulated and measured results for the prototype. The circuit exhibits extremely good performance with a coupling level of $10 \pm 0.6\,\mathrm{dB}$ and insertion loss of less than $1.35\,\mathrm{dB}$, very close to the simulated results in a decade of operational bandwidth (from 1.2 to 12 GHz). Furthermore, it shows a return loss better than 23 dB and an isolation better than 28 dB, as depicted in Figure 11(b). These results clearly outperform previously designed weakly coupled directional couplers in terms of fractional bandwidth and performance [2, 4–6] and demonstrate the validity of the proposed technique to design directional couplers with features comparable (in planar technologies) only with those achievable by homogenous TEM couplers.

4. DESIGN AND EVALUATION OF A THREE-SECTION SLOT-COUPLED QUADRATURE HYBRID

Broadband quadrature hybrids are among the most important microwave passives. They are used in many microwave subsystems such as balanced amplifier, mixers, modulators, beamforming networks, etc.. In most of these applications the amplitude and phase imbalances of the quatrature hybrid are critical and must be minimized to obtain a proper performance.

In this type of wideband tightly coupled structures, the parasitic effects of discontinuities between sections and the difference between phase velocities of even and odd modes are equally important. This was already noticed in [16] where these detrimental effects where partially mitigated by properly adjusting the geometrical parameters (W_i, S_i, and L_i). Although good results were obtained, the isolation and phase imbalance at the end of the UWB band were degraded to 17 dB and 3°, respectively. In this section, it will be shown that these results can be greatly improved using the corrugated slot technique shown in Section 3 to equalize the even and odd mode phase velocities. A three-section slot-coupled quadrature hybrid will be presented which attains an isolation and phase error better than 26 dB and 0.7°, respectively in the complete UWB band of 3.1–10.6 GHz.

According to the 2-D modal analysis of Figure 3, the specific impedances for this design and the coupling level of each section (included in [21]) are obtained (see Table 4). Using these impedance values, the width of the tracks (W_i) and slots (S_i) for each section can be calculated.

Once the initial cross-sectional values have been obtained, the corrugations are introduced in the slot to equalize the even and odd mode phase velocities (as explained in Section 3). However, in this specific design the reactive effect of the discontinuities makes the design more complicated. Effectively, in this circuit there are large differences between the coupling levels of the sections (-1.56 dB and -15.26 dB). Such differences cause an important reactive effect in the discontinuities and increase the electrical length of the even mode.

In order to overcome this problem, a linear transition between

Table 4. Even-odd mode impedances and coupling levels for the three-secion symmetric 3 dB quadrature hybrid [22].

Section	Z_{0e} (Ω)	Z_{0o} (Ω)	C (dB)
1, 3	59.52	42	-15.26
2	167	14.97	-1.56

Table 5. Physical dimensions of the three-section quadrature hybrid.

Section	W (mm)	S (mm)	L (mm)	D (μm)	Λ (μm)
1, 3	0.89	0.79	6.25	-	-
2	3.55	6.45	6.05	400	200
$L_{\text{transition}} = 0.39$ mm					

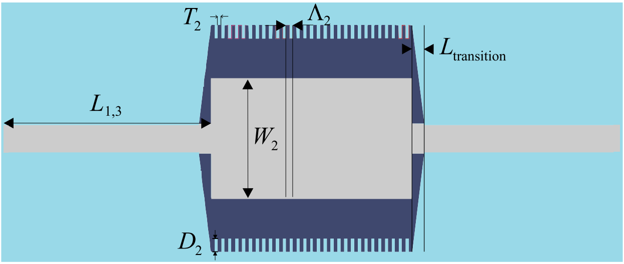

Figure 12. Detailed plot of the upper track (purple) and the corrugated slot (orange) with linear transitions between the central an the outer sections in the three-section quadrature hybrid.

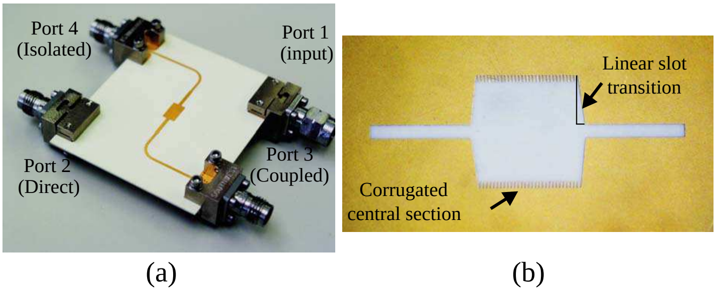

Figure 13. (a) Photograph of the three-section quadrature hybrid. (b) Photograph of the slot showing the corrugations, used to equalize mode phase velocities, and the linear slot transition, used to compensate discontinuity parasitics.

the central and the outer sections is introduced in the slot to reduce the length of the outer section for the even mode without affecting to the odd mode, as depicted in Figure 12. It has been observed that, once the mode phase velocities have been equalized by means of the corrugated slot, the length of this transition ($L_{\text{transition}}$) is easily found out by optimization. The final dimensions used for this circuit are included in Table 5.

A prototype of this circuit has been manufactured using the same symmetrical multilayer stack as the one used for the 10 dB directional coupler. A photograph of the fabricated directional coupler and its novel corrugated slot are shown in Figure 13. This prototype has been measured and the results are shown in Figures 14 and 15. This circuit has exhibited a return loss better than 22 dB and an isolation better than 26 dB from 3.1 to 10.6 GHz (see Figure 14(b)). Focusing in the hybrid imbalances, it is observed that the amplitude imbalance between

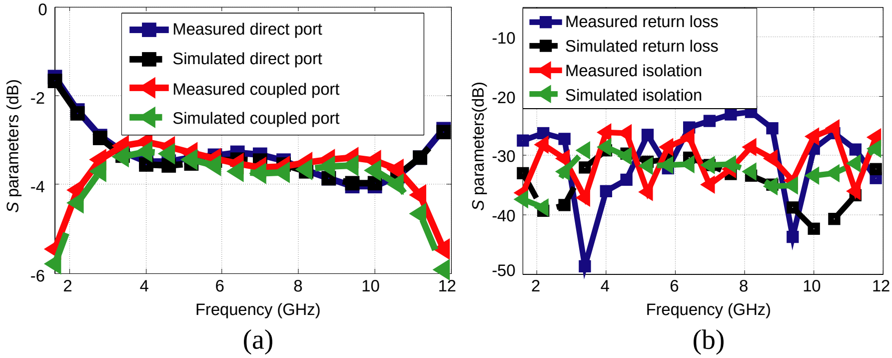

Figure 14. Measured and simulated performance of the fabricated three-section quadrature hybrid. (a) Through and coupled ports. (b) Return loss and isolation.

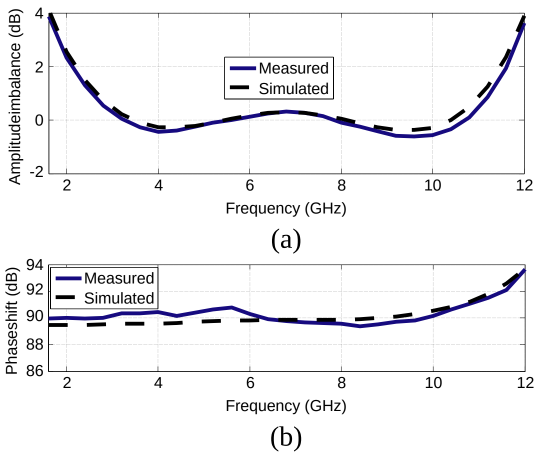

Figure 15. a) Amplitude imbalance between through and coupled ports in the hybrid coupler. (b) Phase shift between through and coupled ports in the hybrid coupler.

output ports is smaller than ± 0.5 dB (see Figure 15(a)), and the phase shift is better than $90 \pm 0.7°$ (see Figure 15(b)). These results clearly outperforms previously reported designs [3, 7, 16–18].

5. CONCLUSIONS

In this paper a new technique for the design high performance directional couplers has been presented. This technique is based on the concept of wiggly coupled lines but applied to the design of slot-coupled directional couplers. In so doing, a new corrugated slot is used enabling almost perfect compensation of even-odd mode phase velocities. This new slot is based on a periodic structure that can be efficiently designed by simulating of only one unit cell (Bloch-Floquet theory) with remarkably accurate results. Even though the proposed technique may require a more complex multilayer structure than wiggly coupled lines, this new technique overcomes all the disadvantages of its counterpart, thus offering i) tighter coupling levels, ii) phase velocity compensation completely transparent between both modes, and iii) a wider range of valid substrates, since high dielectric constant substrates are not required for making circuit fabrication feasible.

To demonstrate the validity of the proposed technique, the design and evaluation of two high performance directional couplers has been carried out. The first one is a 10 dB asymmetric directional coupler that has exhibited a really good coupling accuracy of 10 ± 0.6 dB, a return loss better than 23 dB and an isolation better than 28 dB from 1.2 to 12 GHz. The second one is a symmetric quadrature hybrid that has exhibited a return loss better than 22 dB, an isolation better than 26 dB and extremely small amplitude and phase imbalances of less than ± 0.5 dB and ± 0.7 from 3.1 to 10.6 GHz. These results outperforms previously reported designs and are comparable (in planar technologies) only with those attainable by homogenous TEM couplers.

ACKNOWLEDGMENT

This work has been founded by Andalusian Regional Ministry of Science, Innovation and Business under projects P09-TIC-5268, MUPHY and a FPDI scholarship (780008), and by AT4wireless under the contract 8.06/5.59.3165.

REFERENCES

1. Lopez-Berrocal, B., J. de-Oliva-Rubio, E. Marquez-Segura, A. Moscoso-Martir, and I. Molina-Fernandez, "High performance 1.8–18 GHz 10-dB low temperature co-fired ceramic directional coupler," *Progress In Electromagnetics Research*, Vol. 104, 99–112, 2010.
2. Kim, C.-S., S.-W. Lee, P.-Y. Lee, H.-S. Kim, J.-S. Park, and D. Ahn, "Design of re-entrant mode microstrip directional coupler for high directivity performance," *IEEE Asia-Pacific Microwave Conference*, 1286–1289, Dec. 2000.
3. Sharma, R. Y., T. Chakravarty, S. Bhooshan, and A. B. Bhattacharyya, "Design of a novel 3 dB microstrip backward wave cou-

pler using defected ground structure," *Progress In Electromagnetics Research*, Vol. 65, 261–273, 2006.

4. Phromloungsri, R., M. Chongcheawchamnan, and I. D. Robertson, "Inductively compensated parallel coupled microstrip lines and their applications," *IEEE Trans. on Microw. Theory and Tech.*, Vol. 54, No. 9, Sep. 2006.
5. Moradian, M. and M. Khalaj-Amirhosseini, "Improvement the characteristics of the microstrip parallel coupled line coupler by means of grooved substrate," *Progress In Electromagnetics Research M*, Vol. 3, 205–215, 2008.
6. Pelaez-Perez, A. M., P. Almorox-Gonzalez, J. I. Alonso, and J. Gonzalez-Martin, "Ultra-broadband directional couplers using microstrip with dielectric overlay in millimeter-wave band," *Progress In Electromagnetics Research*, Vol. 117, 495–509, 2011.
7. Chen, H.-C. and C.-Y. Chang, "Modified vertically installed planar couplers for ultrabroadband multisection quadrature hybrid," *IEEE Microw. and Wireless Compon. Lett.*, Vol. 16, No. 8, 446–448, Aug. 2006.
8. Gruszczynski, S. and K. Wincza, "Broadband rat-race couplers with coupled-line section and impedance transformers," *IEEE Microw. Wireless Compon. Lett.*, Vol. 22, No. 1, 22–24, Jan. 2012.
9. Izydorczyk, J., "Equivalent circuits for nonuniform transmission line simulation," *ACES Journal*, Vol. 25, No. 9, 764–779, Sep. 2010.
10. Khalaj-Amirhosseini, M., "Analysis of coupled or single nonuniform transmission lines using step-by-step numerical integration," *Progress In Electromagnetics Research*, Vol. 58, 187–198, 2006.
11. Uysal, S. and A. H. Aghvami, "Synthesis, design an construction of ultra-wide-band nouniform quadrature directional coupler in inhomogeneous media," *IEEE Trans. on Microw. Theory and Tech.*, Vol. 37, No. 6, 969–976, 1989.
12. Podell, A., "A high directivity microstrip coupler technique," *IEEE MITS Int. Microwave Symp. Dig.*, 33–36, 1970.
13. Lau, D. K. Y., S. P. Marsh, L. E. Davis, and R. Sloan, "Simplied design technique for high-performance microstrip multisection couplers," *IEEE Trans. on Microw. Theory and Tech.*, Vol. 46, No. 12, 2507–2512, Dec. 1998.
14. Muller, J. and A. F. Jacob, "Advanced characterization and design of compensated high directivity quadrature coupler," *IEEE MITS Int. Microwave Symp. Dig.*, 724–727, 2010.
15. Tanaka, T., K. Tsunoda, and M. Aikawa, "Slot-coupled

directional couplers between double-sided substrate microstrip lines and their applications," *IEEE Trans. on Microw. Theory and Tech.*, Vol. 36, No. 12, 1752–1757, Dec. 1988.

16. Moscoso-Martir, A., J. G. Wangemert-Perez, I. Molina-Fernandez, and E. Marquez-Segura, "Slot-coupled multisection quadrature hybrid for UWB applications," *IEEE Microw. Wireless and Compon. Lett.*, Vol. 19, No. 3, 143–145, Mar. 2009.
17. Abbosh, A. M. and M. E. Bialkowski, "Design of ultra wideband 3 dB quadrature microstrip/slot coupler," *Microw. Opt. Tech. Lett.*, Vol. 49, No. 9, 2101–2103, Sep. 2007.
18. Nedil, M. and T. A. Denidni, "Analysis and design of an ultra wideband directional coupler," *Progress In Electromagnetics Research B*, Vol. 1, 291–305, 2008.
19. Moscoso-Martir, A. and I. Molina-Fernandez, "Six-port junction with complete UWB band coverage in multilayer technology," *IEEE European Microwave Conference (EuMC)*, 655–658, Manchester, Great Britain, 2011.
20. Levy, R., "Tables for asymmetric multi-element coupled transmission-line directional couplers," *IEEE Trans. on Microw. Theory and Tech.*, Vol. 12, 275–279, 1964.
21. Cristal, E. G. and L. Young, "Theory and tables of optimum symmetrical TEM-mode coupled-transmission-line directional couplers," *IEEE Trans. on Microw. Theory and Tech.*, Vol. 13, No. 5, 544–558, Sep. 1965.
22. Monghia, R., I. Bahl, and P. Bhartia, *RF and Microwaves Coupled-line Circuits,* Artech House 1999.
23. Bockelman, D. E. and W. R. Eisenstadt, "Combined differential and common-mode scattering parameters," *IEEE Trans. on Microw. Theory and Tech.*, Vol. 43, No. 7, 1530–1539, Jul. 1995.
24. Fan, W., A. Lu, L. Wai, and B. Lok, "Mixed-mode S-parameter characterization of differential structures," *5th Conference Electronics Packaging Technology (EPTC 2003)*, 533–537, 2003.
25. Wong, M. F., V. F. Hanna, O. Picon, and H. Baudrand, "Analysis and design of slot-couplers between double-sided substrate microstrip lines," *IEEE Trans. on Microw. Theory and Tech.*, Vol. 29, No. 12, 2123–2129, Dec. 1991.
26. Pozar, D. M., *Microwave Engineering Reading,* Addison-Wesley, MA, 1990.
27. Collin, R. E., *Foundations for Microwave Engineering,* 2nd edition, McGraw-Hill, New York, 1992.